CHAPTER IV

Chitosan, poly(lactic-co-glycolic acid), and poly(α-butyl cyanoacrylate) micro-/nanoparticles intended for cellular delivery of protein: Physicochemical properties, cytotoxicity and cellular uptake in dendritic cells and macrophages

Introduction

Many biopharmaceuticals, both peptide-/protein-based and nucleic acid-based, need to be trafficked into the correct intracellular compartment, in order to bind with their targets and subsequently express their activity. DNA first needs to escape endosomal compartment before it can enter into further steps towards transcription to the encoded proteins. Antisense oligonucleotides must reach distinct compartments inside the cell such as the cytosol and/or nucleus and interact with the target mRNA to exhibit an antisense effect. Furthermore, the delivery of exogenous antigens to professional antigen presenting cells is mandatory for vaccine therapeutics. To fulfill these purposes, efficient delivery systems are essentially needed.

Numerous polymeric micro-/nanoparticles have shown a certain degree of success for the delivery of drugs and proteins to the systemic circulation or to the target site (Carino, Jacob and Mathiowitz, 2000; Ko *et al.*, 2002). Of those, the biodegradable polyesters, poly(lactic acid) and poly(lactic-co-glycolic acid), are the primary candidates (Blanco and Alonso, 1997; Tobio *et al.*, 1998; Youan, 2004), since they have been used in humans for many years as suture materials and as controlled release drug delivery systems. Others included chitosan (He, Davis and Illum, 1999; Ko *et al.*, 2002; Shu and Zhu, 2001, 2002), poly(ε-caprolactone) (Youan, 2004), poly(α-butyl cyanoacrylate) (Behan and Birkinshaw, 2001), etc.

This study was aimed to investigate the potential of chitosan microparticles as delivery systems for targeting antigenic proteins to antigen presenting cells. Bovine serum albumin was used as a model antigenic protein. For comparison, poly(lactic-co-glycolic acid) and poly(α-butyl cyanoacrylate) micro-/nanoparticles were also

investigated. In addition to physicochemical characteristics, the particles were characterized by their interaction with dendritic cells and macrophages.

Materials and methods

Materials

Chitosan at molecular weight of 37 kDa with 94% degree of deacetylation (LCS) and 100 kDa with 95% degree of deacetylation (HCS) were obtained from Seafresh Chitosan (Bangkok, Thailand). Chitosan of different source (Flonac C, molecular weight of 50-100 kDa and 90.7% degree of deacetylation) (JCS) was provided by Kyowa Technos (Japan). Bovine serum albumin, Cohn Fraction V (BSA) was purchased from Sigma-Aldrich (Saint Louis MO, USA). Gelatin (GEL) was supplied from Fluka Chemie (Buchs, Switzerland). Poloxamer 407 (Lutrol F 127) (POL) and poly(butyl methacrylate, [2-dimethyl aminoethyl] methacrylate, methyl methacrylate), 1:2:1 (Eudragit EPO) (EUD) were obtained as gifts from BASF (Florham Park NJ, USA) and Röhm (Darmstadt, Germany), respectively. Poly(lactic-co-glycolic acid), 50:50 with inherent viscosity of 0.37 dl/g in hexafluoro isopropanol (PLGA) was purchased from Absorable Polymers International (Pelham AL, USA). Alpha-butyl cyanoacrylate monomer (Compont) (BCA) was received as gift from Beijing Suncon Medical Adhesive (Beijing, China). All other chemicals were of analytical grade and used as received.

Methods

Preparation of chitosan microparticles

Chitosan was dissolved in 0.5% acetic acid solution and spray dried in a bench-top spray dryer (Büchi model 190, Büchi Labortechnik, Flawil, Switzerland). The liquid feed was pumped peristaltically and fed through a two-fluid nozzle (0.5 mm internal diameter) where it was atomized into fine droplets. Cooling water was circulated through the jacket around the nozzle throughout the process. The standard processing parameters comprised an atomizing air volumetric flow rate of 750 l/hr and the aspirator vacuum of 25 mbar. The inlet drying air temperature and the liquid feed rate were controlled at 120 ^{o}C and 3 ml/min, respectively. Since it was not possible to control the outlet air temperature, it was thus only observed. To incorporate either BSA or other excipients into microparticles, the material was first

dissolved in a certain volume of distilled water, subsequently mixed with chitosan solution, in a manner that the final concentration of all components was controlled, and spray dried as described above. For cross-linking, chitosan microparticles were dispersed in a few milliliters of absolute ethanol and sonicated with a 3-mm-tip diameter standard probe at output control of 60 (Vibra Cell model VC 130 PB, Sonics and Materials, Newtown CT, USA) for about 30 seconds, in order to deaggregate the microparticles. The dispersion was loaded drop-wise and stirred in the 1% w/v tripolyphosphate solution for 30 minutes. After the reaction, the particles were filtered, washed three times with distilled water and subsequently vacuum-dried overnight.

Preparation of poly(lactic-co-glycolic acid) microparticles

BSA and PLGA were separately dissolved in distilled water and dichloromethane, respectively. One part of aqueous phase and five parts of organic phase were mixed together by means of sonication as described above, but at an output control of 100. The mixture was then dispersed into 25 parts of either 1 or 2% w/v polyvinyl alcohol (PVA) solution by means of sonication with a 6-mm-tip diameter standard probe at an output control of 100 for 30 seconds, and subsequently transferred to 50 parts of magnetically stirred either 0.1 or 0.2% w/v PVA solution. The final mixture was kept stirring for 4-6 hours. The particles were separated by centrifugation (Eppendorf model 5810, Eppendorf AG, Hamburg, Germany) at 4000 rpm for 15 minutes, washed three times with distilled water and eventually re-dispersed with distilled water to the original volume of dichloromethane.

Preparation of poly(α-butyl cyanoacrylate) nanoparticles

One hundred microliters of α-butyl cyanoacrylate monomer was added drop-wise into 10 ml of either pH 1 or pH 3 hydrochloric acid solutions and stirred for 4 hours until milky white suspension was obtained. For stabilizer-containing formulations, a required amount of dextran was first dissolved in the aqueous acidic solution prior to the addition of monomer. After the particles were formed, which took about 1 and 4 hour(s) for the polymerization at pH 3 and 1, respectively, pre-

dissolved BSA in 0.5 ml distilled water was added drop-wise into the mixture. The mixture was stirred for another 3-4 hours for complete adsorption of protein.

Particle size measurement

Particle size and size distribution of chitosan and PLGA microparticles were measured by laser light-scattering method (Mastersizer 2000, Malvern Instrument, Malvern, UK). For chitosan microparticles, small amount of particles was first dispersed in a few milliliters of absolute ethanol and sonicated as previously described under the 'preparation of chitosan microparticles' section, in order to deaggregate the microparticles. The particle dispersion was loaded into a stirred sample cell, containing water as a measuring medium. Calculation of particle size was made from the intensity of light scattered at different angles, based on Mie's theory (Zimmerman, 1997). The particle size is presented in the volume-weighted mode and the 50% undersize diameter d (v, 0.5) is referred to as the particle diameter. Particle size and size distribution of BCA nanoparticles were determined by photon correlation spectroscopy (Zetasizer NanoZS, Malvern Instrument, Malvern, UK). Z-average and polydispersity index in the intensity distribution mode were reported as the particle diameter and size distribution, respectively.

Zeta potential measurement

Chitosan microparticles were dispersed in 1 mM NaCl solution with sonication, as described under the 'preparation of chitosan microparticles' section, while other particles were dispersed without sonication. The measurement was carried out on the Zetasizer NanoZS (Malvern Instrument, Malvern, UK). At least 20 sub-runs were performed at room temperature. The results were reported as zeta potential and zeta deviation.

Particle morphology

Chitosan microparticles were mounted onto double-faced adhesive tape, which was attached on a sample stub. PLGA microparticles were filtered and vacuum-dried before being mounted onto the sample stub. The samples were sputtered with gold and viewed under a scanning electron microscope (Jeol model JSM-5410 LV, Tokyo, Japan) at a voltage of 15.0 kV. The photomicrographs were then taken at a

magnification of 7500. BCA nanoparticles were freeze-dried, prepared as described above and viewed under a scanning electron microscope (Jeol model JSM 5600 LV, Tokyo, Japan). The photomicrographs were then taken at a magnification of either 5000 or 10 000.

Surface analysis

The presence of BSA at or near the particle surface was investigated by X-ray photoelectron spectroscopy (XPS Axis-Ultra, Kratos Analytical, UK), using monochromatic Al K_{α} radiation at 225 W and low-energy electron flooding for charge compensation. All C1s hydrocarbon peak were recalibrated at a binding energy of 284.80 eV to compensate for surface charges effects. The percentage of BSA exposed at or near the particle surface was calculated by dividing the percentage of sulfur exposed at the particle surface with that exposed at the surface of BSA and multiplying by 100.

Protein content determination

Chitosan and PLGA microparticles were separately dissolved in 0.5% acetic acid solution and the mixture of 1:1 dimethyl sulfoxide and 0.5% dodecyl sufate in 0.05 N NaOH, respectively. BSA content was determined by using bicinchoninic acid kit for protein determination (Sigma-Aldrich, Saint Louis MO, USA). The reaction was run at room temperature for 2 hours. Optical density of the sample solution was read at 562 nm on a spectrophotometer (Jasco model V-530, Jasco, Tokyo, Japan). Actual protein loading and entrapment efficiency were then calculated. The experiment was performed in triplicate. BCA nanoparticles were separated by centrifugation (Ruijiang model RT-TGL-16 G, Ruijiang Beijing, China) at 15 000 rpm for 30 minutes. The protein content was determined indirectly from the supernatant of the reaction medium, according to Bradford method (Bradford, 1976). Briefly, 200 µl of the sample solution were reacted with 2 ml of Bradford working solution (35 mg of Coomassie brilliant blue dissolved in 25 ml 95% ethanol, 50 ml 88% phosphoric acid and 425 ml distilled water) at room temperature for 2 minutes. Optical density of the sample solution was read at 595 nm on a spectrophotometer (PGeneral model TU-1901, Beijing Purkinje General Instrument, Beijing, China).

Actual protein loading and entrapment efficiency were then calculated. The experiment was performed in triplicate.

In vitro release test

Ten milligrams of micro-/nanoparticles were suspended in 1 ml of pH 7.4 phosphate buffered saline (PBS) and then shaken horizontally 120 rpm at 37 °C. At predetermined time intervals, the supernatant was separated by centrifugation (Eppendorf model 5810, Eppendorf AG, Hamburg, Germany) at 7500 rpm for 10 minutes for the microparticulate samples or as described under the 'protein content determination' section for the nanoparticulate samples and assayed for the protein released as described above. The experiment was carried out in triplicate.

Protein integrity

Sodium dodecyl sulfate-polyacrylamide gel electrophoresis (SDS-PAGE) BSA was recovered by dissolving microparticles as described under the 'protein content determination' section. BCA nanoparticles were shaken with distilled water at room temperature overnight. The supernatant, as the sample solution, was separated and assayed as described above. One part of the samples was mixed with one part of reducing sample buffer (5% β-mercaptoethanol in Novex® Tris-Glycine SDS sample buffer; Invitrogen, Calsbad CA, USA) and heated at 95 °C for 1 minute. The mixture equivalent to 7.5 μg of BSA was then loaded onto a pH 8.8 12% Bis-Tris polyacrylamide gel and subjected to electrophoresis (Bio-Rad model Mini-PROTEAN II, Bio-Rad Laboratories, Hercules CA, USA) in pH 8.3 Novex® Tris-Glycine SDS running buffer (Invitrogen, Calsbad CA, USA) at 80 V for about 2 hours. The gel was stained with SimplyBlue™ SafeStain (Invitrogen, Calsbad CA, USA) for 1 hour and destained several times with distilled water until the protein bands were visualized.

Circular dichroism (CD) BSA was recovered from the micro-/nanoparticles as described above. Sample solutions were diluted with ultrapure water to obtain about 50 μg/ml of BSA in solution. Ellipticity (θ, mdeg) of the solutions was recorded between 190-350 nm on a spectropolarimeter (Jasco model J-715, Jasco,

Tokyo, Japan). Molar ellipticity ($[\theta]$, deg cm^2/decimol) was then calculated by the following equation

$$[\theta] = \theta \, Mp / 10\,000 \, n \, C^* \, l \qquad (1)$$

where Mp is molecular weight of BSA (66 430 Da), n is number of amino acid residues of BSA (583 residues), C* is concentration of BSA in sample solution (g/ml) and l is path length of cell (0.5 cm). CD spectra were obtained by plotting molar ellipticity against wavelength. The solution of corresponding blank microparticles of each sample was prepared as described above and run as background.

Cytotoxicity study

Mouse dendritic cells (DC) (ATCC CRL-11904) and mouse splenic macrophages (Mϕ) (ATCC CRL-2471) at concentration of $5x10^5$ cells in 100 µl complete culture medium were separately seeded into each well of 96-well plates and incubated at 37 °C with 5% CO_2 in air atmosphere for 24 hours. After cells had settled, the particles at varying loading in 100 µl pH 7.4 PBS were co-incubated with cells for another 24 hours at the same condition. Mitochondrial activity of viable cells was measured by Alamar Blue assay. Fifteen microliters of the reagent were added into each well and incubated at 37 °C for four hours. Percentage of cell viability was calculated by comparing the fluorescence intensity at the excitation wavelength of 540 nm and the emission wavelength of 590 nm (VICTOR^3, Perkin Elmer, USA) of the samples with that of the negative control (cells co-incubated with pH 7.4 PBS), which was considered as 100% viability. The corresponding complete culture medium was also run as blank.

In vitro cellular uptake

DC and Mϕ at concentration of $4x10^6$ cells in 2 ml complete culture medium were seeded in 6-well plate and incubated at 37 °C with 5% CO_2 in air atmosphere until the cell confluency was reached. BSA and the non-toxic chitosan and BCA micro-/nanoparticles were labeled with fluorescein-5-isothiocyanate, isomer I (FITC) (Invitrogen, Calsbad CA, USA), according to the manufacturer's information. For

PLGA microparticles, BSA was first labeled by the same procedure and subsequently incorporated into the microparticles. The FITC-labeled micro-/nanoparticles at non-toxic loading were co-incubated with cells for another four hours at the same condition. The particle uptake was analyzed with a fluorescence-activated cell sorter (FACS) (BD model FACSCalibur, BD Biosciences, San Jose CA, USA), equipped with argon laser. The fluorescence signal was detected with G1 detector for green fluorescence signal at the excitation wavelength of 485 nm and the emission wavelength of 525 nm. The number of fluorescence event, which correlated to the particles taken up within the cells, was counted. The gated cells with fluorescence signal were defined as the positive cells for cellular uptake. The percentage of positive cells relative to the control experiment (cells co-incubated with FITC solution) was then determined.

Results

Physicochemical properties and morphology of micro-/nanoparticles

Chitosan and chitosan composite microparticles for cellular delivery of protein were prepared by spray drying technique. Physicochemical characteristics of the resultant microparticles are shown in Table 4.1. The number in the nomenclature of microparticles designated the concentration as percent by weight of the excipients incorporated into the microparticles.

The particle size and size distribution, indicated by uniformity, of all blank chitosan microparticles were ranged between 2.979-5.450 μm and 0.258-0.652 μm, respectively. The particles obviously exposed positive surface charge. It was found that JCS microparticles exhibited slightly higher zeta potential than LCS and HCS microparticles. Co-spray drying of GEL along with chitosan induced a remarkable increase in zeta potential of microparticles, while that of POL and EUD did not affect the zeta potential significantly.

Compared with the corresponding blank microparticles, the protein-loaded micropaticles were slightly larger, with similar size distribution. Incorporation of BSA into microparticles resulted in a comparable or slight decrease in zeta potential,

except the GEL composite microparticles, the zeta potential of which was decreased apparently. The protein loading and the protein entrapment efficiency were ranged between 2.55-4.67 and 50.05-86.72%, respectively. It was noticed that the loading and the entrapment efficiency of GEL composite microparticles were lower than those of the others.

Morphology and topography of chitosan and chitosan composite microparticles are illustrated in Figures 4.1 and 4.2.

The blank chitosan microparticles of different molecular weights and/or sources were relatively spherical, with dented surface, the highest degree of which was seen on the HCS microparticles (Figures 4.1A-4.1C). Encapsulation of protein yielded a slightly rougher surface than the original particles (Figures 4.1D-4.1F).

Inclusion of excipients into chitosan microparticles considerably changed morphology and topography of the particles in different ways. The GEL composite microparticles had less dented, but more undulate surface than the LCS microparticles (Figures 4.2A and 4.1A). Addition of POL resulted in the microparticles with a smoother surface. It was noted that some particles were fused together, leading to an agglomeration of the particles (Figure 4.2B). As shown in Figure 4.2C, EUD could eliminate most of dents on the particle surface, yielding the microparticles with smoother, but matte surface. All of the effects were more pronounced as the concentration of the excipients in microparticles was increased (photomicrographs not shown). The composite microparticles became dented and undulate, once BSA was incorporated into the particles (Figures 4.2D-4.2F). Some distorted particles were also found in these cases. In addition, modification of HCS and JCS microparticles by co-spray drying with the excipients resulted in the similar effects to those of the LCS microparticles (photomicrographs not shown).

The LCS microparticles were further modified by cross-linking in 1% w/v tripolyphosphate solution at pH 5 and 9. The physicochemical properties and morphology of microparticles are presented in Table 4.2 and Figure 4.3, respectively.

Table 4.1 Physicochemical properties of chitosan and chitosan composite microparticles

	Blank microparticles		BSA-loaded microparticles			
	Size (μm)	Zeta potential (mV)	BSA loading (%)	EE* (%)	Size (μm)	Zeta potential (mV)
LCS	3.427 (0.358)**	24.97 (3.400)***	4.34 (0.08)***	86.72	4.510 (0.473)	23.10 (7.258)
5 GEL LCS	3.736 (0.258)	35.10 (3.209)	3.36 (0.22)	67.73	4.778 (0.562)	32.58 (3.388)
15 GEL LCS	4.120 (0.261)	37.18 (3.537)	2.55 (0.61)	50.05	4.286 (0.567)	29.58 (10.89)
25 GEL LCS	3.651 (0.322)	36.20 (3.632)	2.90 (0.44)	56.20	4.628 (0.542)	29.86 (5.707)
5 POL LCS	3.370 (0.382)	26.99 (7.234)	4.21 (0.07)	83.86	4.673 (0.419)	25.32 (6.000)
15 POL LCS	3.110 (0.340)	24.99 (14.81)	3.89 (0.07)	78.33	4.348 (0.465)	23.35 (7.459)
25 POL LCS	3.109 (0.326)	25.67 (11.26)	4.01 (0.11)	80.22	4.304 (0.604)	20.40 (8.483)
5 EUD LCS	4.685 (0.652)	23.60 (5.692)	4.56 (0.16)	82.98	5.622 (0.531)	21.76 (4.661)
15 EUD LCS	3.383 (0.530)	27.02 (6.128)	4.50 (0.18)	81.88	4.324 (0.544)	21.95 (6.595)
25 EUD LCS	2.979 (0.394)	25.74 (11.11)	4.53 (0.06)	82.73	3.185 (0.545)	23.19 (8.124)

*Entrapment efficiency

**Absolute deviation from the median (Uniformity)

***Standard deviation

Table 4.1 Physicochemical properties of chitosan and chitosan composite microparticles (continued)

	Blank microparticles		BSA-loaded microparticles			
	Size (μm)	Zeta potential (mV)	BSA loading (%)	EE* (%)	Size (μm)	Zeta potential (mV)
HCS	3.899 (0.346)**	23.70 (4.159)***	3.48 (0.74)***	72.49	5.964 (0.455)	23.22 (6.717)
15 GEL HCS	4.468 (0.509)	33.04 (5.589)	2.83 (0.16)	56.89	6.704 (0.292)	33.41 (3.578)
15 POL HCS	3.395 (0.358)	25.94 (11.09)	3.98 (0.39)	80.12	6.104 (0.448)	25.19 (4.599)
15 EUD HCS	3.049 (0.385)	25.34 (10.64)	4.37 (0.05)	79.75	3.805 (0.505)	26.09 (7.816)
JCS	5.450 (0.284)	29.12 (3.831)	3.75 (0.03)	75.12	7.177 (0.586)	23.09 (4.186)
15 GEL JCS	5.330 (0.286)	39.82 (3.986)	3.28 (0.47)	65.98	4.841 (0.421)	29.35 (3.898)
15 POL JCS	4.360 (0.370)	24.68 (7.041)	4.22 (0.61)	83.79	5.227 (0.404)	22.80 (4.817)
15 EUD JCS	3.615 (0.462)	28.01 (9.131)	4.67 (0.25)	84.18	5.039 (0.466)	22.13 (4.848)

*Entrapment efficiency

**Absolute deviation from the median (Uniformity)

***Standard deviation

Table 4.2 Physicochemical properties of crosslinked chitosan and chitosan composite microparticles

	Blank microparticles		BSA-loaded microparticles			
	Size (μm)	Zeta potential (mV)	BSA loading (%)	EE* (%)	Size (μm)	Zeta potential (mV)
C LCS pH 5	4.292 (0.583)**	18.03 (7.109)***	3.57	-	4.958 (0.521)	16.33 (9.518)
C LCS pH 9	4.292 (0.583)	18.03 (7.109)	3.31	-	9.037 (1.000)	12.75 (5.915)
C 15 GEL LCS	14.885 (0.690)	13.07 (5.333)	1.52	-	19.797 (3.670)	15.74 (5.594)
C 15 POL LCS	-	-	4.19	-	3.126 (0.814)	20.87 (10.72)
C 15 EUD LCS	4.176 (0.549)	27.01 (6.145)	4.08	-	3.137 (0.944)	32.57 (11.53)

*Entrapment efficiency

**Absolute deviation from the median (Uniformity)

***Standard deviation

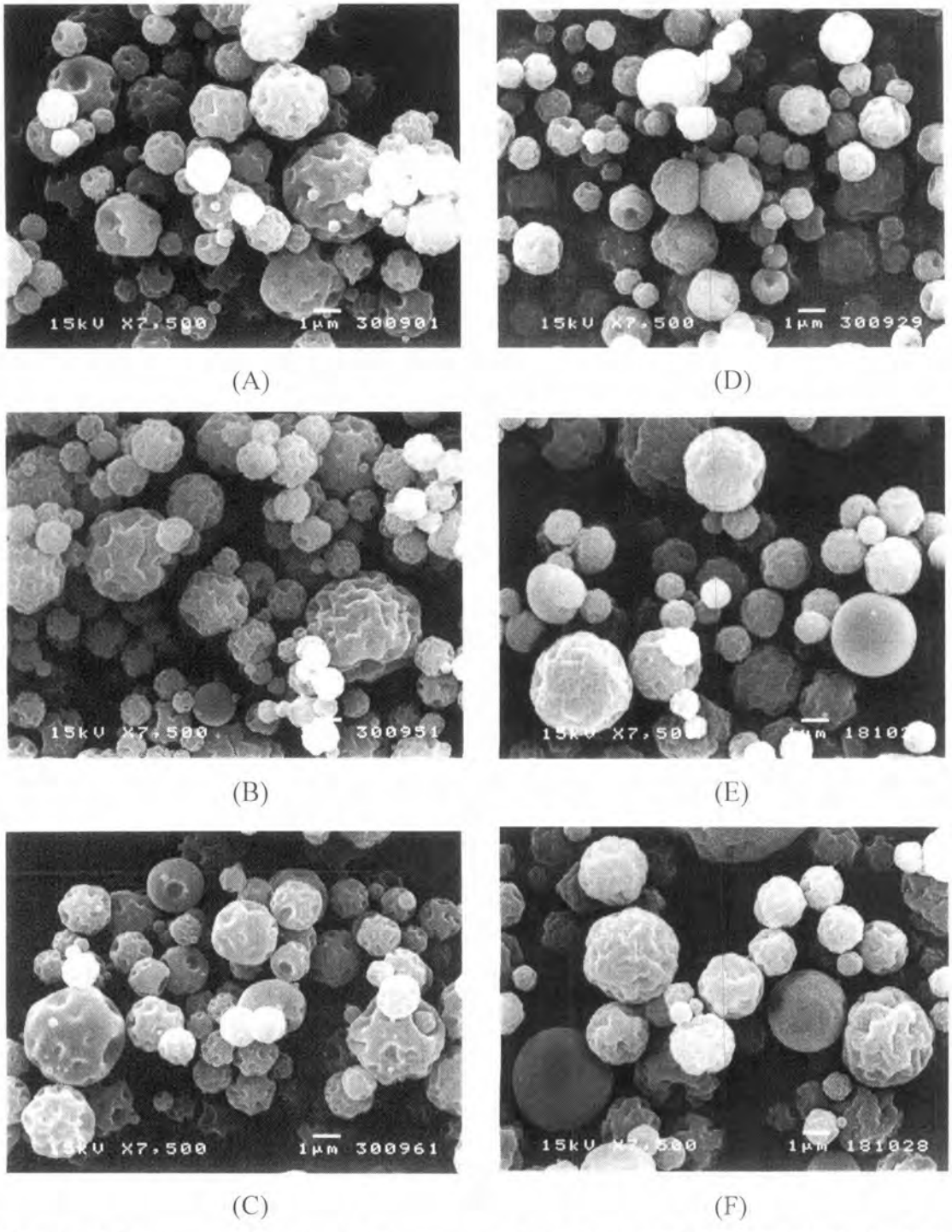

Figure 4.1 Scanning electron photomicrographs of blank (A) LCS, (B) HCS, (C) JCS, and BSA-loaded (D) LCS, (E) HCS, and (F) JCS microparticles

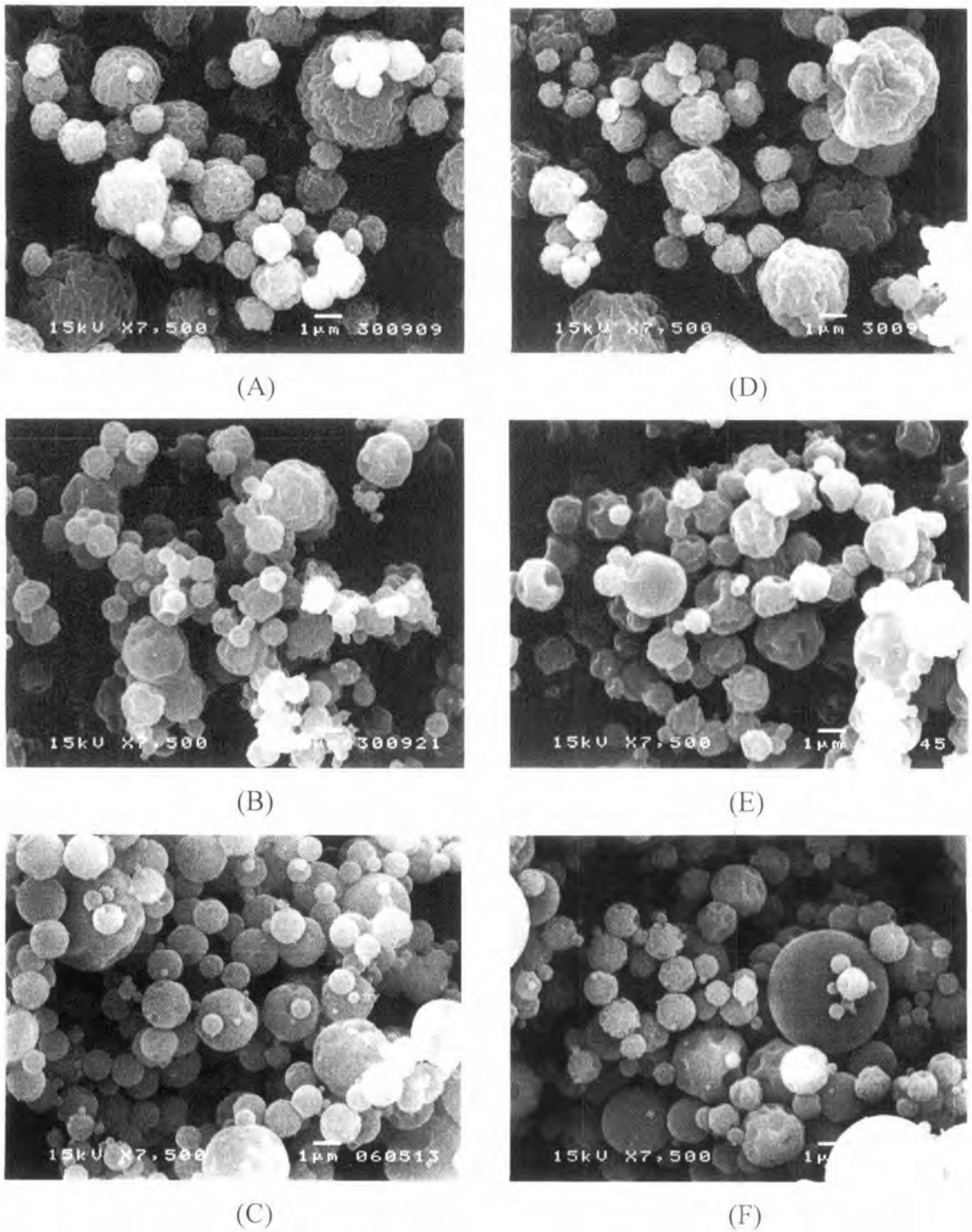

Figure 4.2 Scanning electron photomicrographs of blank LCS microparticles, co-spray dried with 15% w/w of (A) GEL, (B) POL, (C) EUD, and BSA-loaded LCS microparticles, co-spray dried with 15% w/w of (D) GEL, (E) POL, and (F) EUD

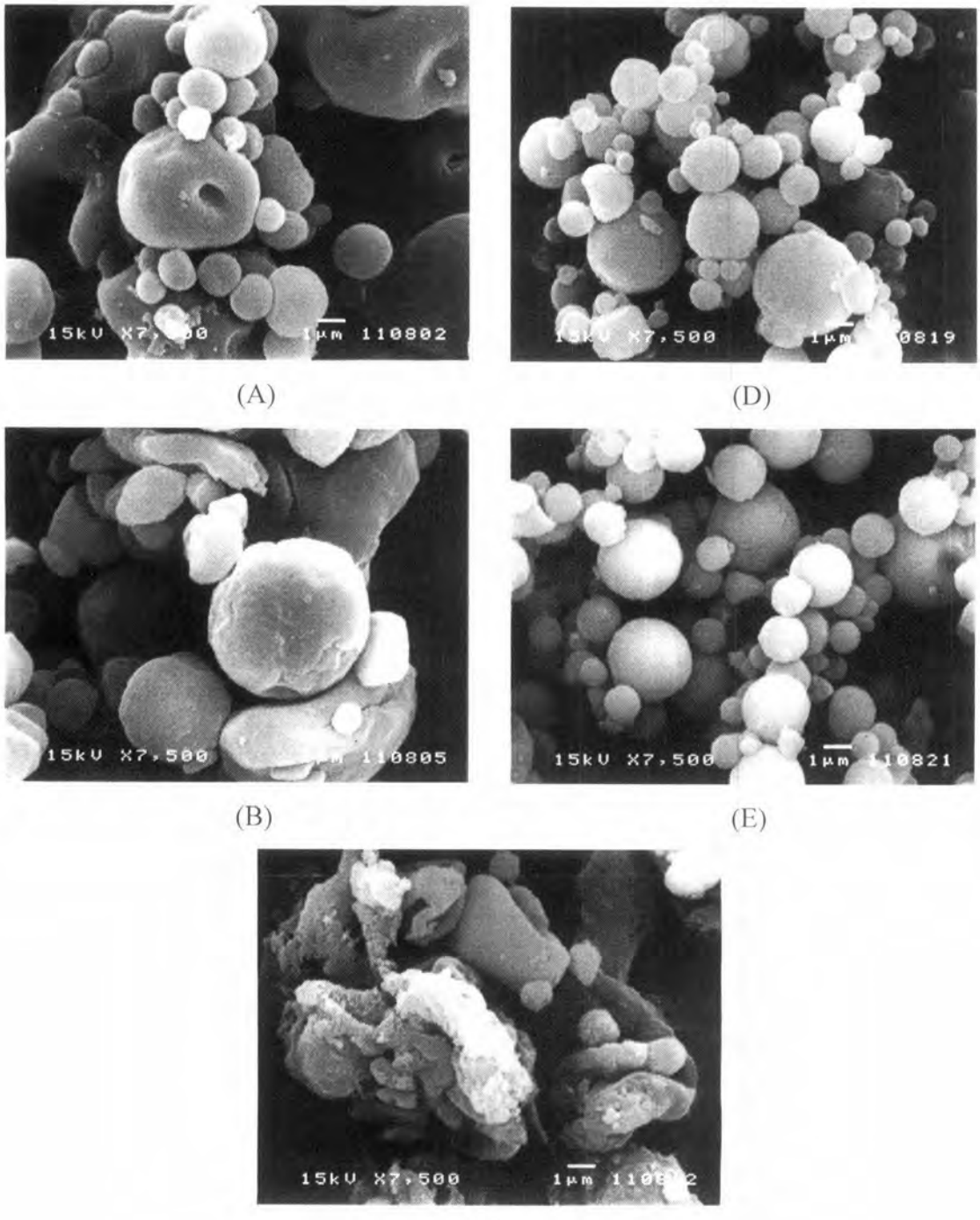

Figure 4.3 Scanning electron photomicrographs of BSA-loaded LCS microparticles, crosslinked in 1% w/v tripolyphosphate solution at (A) pH 5, (B) pH 9, BSA-loaded (C) 15 GEL LCS, (D) 15 POL LCS, and (E) 15 EUD LCS microparticles, crosslinked in 1% w/v tripolyphosphate solution at pH 5

Cross-linking of blank and BSA-loaded LCS microparticles at pH 5 yielded the microparticles, with comparable in size to, but slightly larger in size distribution

than the original particles, whereas the processing at pH 9 caused about doubly larger microparticles. However, zeta potential of the crosslinked microparticles was reduced dramatically. The processed microparticles had very smooth surface, especially those prepared at lower pH. Some distorted particles were also found (Figures 4.3A and 4.3B).

Taking into account the LCS composite microparticles, which were crosslinked at pH 5, the GEL-containing microparticles, both blank and BSA-loaded, were much larger than their original particles. The observation under an electron microscope revealed some agglomeration of many distorted particles (Figure 4.3C). It was found that the cross-linking process caused a substantial decrease in zeta potential of the microparticles. In contrast, the particle size of POL and EUD composite microparticles before and after the cross-linking process were comparable. While zeta potential of the POL composite microparticles was maintained, that of the EUD composite microparticles was increased after the procedure. Both crosslinked particles were spherical, with very smooth surface (Figures 4.3D and 4.3E). Additionally, the modification process resulted in a slight decrease of protein loading in most cases, except the POL composite microparticles, the BSA loading of which was slightly increased from 3.89 to 4.19%.

PLGA microparticles were prepared by double-emulsion solvent-evaporation technique at two different concentrations of PVA. The properties and morphology of particles are illustrated in Table 4.3 and Figure 4.4, respectively.

Blank PLGA microparticles were relatively small, when compared with the chitosan microparticles. Upon BSA incorporation, the microparticles became much larger, both in size and size distribution, than the BSA-loaded chitosan microparticles. The actual protein loading and entrapment efficiency were satisfactorily high and reached 99% as the concentration of PVA was increased. PLGA microparticles were relatively neutral, with a slightly negative zeta potential. It was evident that both blank and BSA-loaded PLGA microparticles were clearly spherical, with a very smooth surface. Encapsulation of protein resulted only in larger size, without any effect on the surface topography of the particles. Additionally, preparation of

microparticles at different concentrations of PVA yielded the microparticles with similar morphology (photomicrographs not shown).

BCA nanoparticles were prepared by anionic polymerization method at two levels of pH and different concentrations of dextran, used as a stabilizer. The properties and morphology of nanoparticles are shown in Table 4.4 and Figure 4.5, respectively. The number before and after period in the designation of nanoparticles indicated the polymerization pH and the concentration of stabilizer that applied, respectively. In some cases, the number coming after a hyphen indicated the polymerization time at which the BSA was loaded onto the nanoparticles.

Polymerization at pH 3 yielded the comparable-sized nanoparticles, with a narrow size distribution, independent of the concentration of dextran applied. However, zeta potential of the particles decreased, as the concentration of dextran in the polymerization medium was increased. Upon addition of protein, the nanoparticles were slightly larger in size than the corresponding blank nanoparticles, along with a slightly reduced zeta potential.

In case of the particles prepared at pH 1, the stabilizer played a very important role on the success of the preparation process and hence the properties of the resultant nanoparticles. Without dextran, the formed particles became agglomerated together as white material floating on the surface of polymerization medium. The nanoparticles could be collected only when dextran was added into the preparation medium. It was found that the nanoparticles obtained were larger in size than those prepared at higher pH. The particle size was reduced as the dextran concentration was increased. The smallest size of 296 nm was obtained at the concentration of stabilizer as high as 30%. In contrast to the polymerization at pH 3, increasing the concentration of dextran did not affect the zeta potential of particles. Two parameters were found to influence the properties of BSA-loaded nanoparticles, *i.e.* the stabilizer concentration and the polymerization time, at which BSA was loaded onto the particles. Much larger particles than the corresponding blank nanoparticles were obtained, when the nanoparticles were prepared at 5 and 10% w/v dextran and loaded with BSA at hour 4 and hour 2 of polymerization, respectively. In contrast, the

smaller particles of 161-230 nm were received, when the nanoparticles were prepared at 10 and 20% w/v dextran and/or loaded with BSA at hour 3 or 4 of polymerization. Interestingly, the zeta potential of nanoparticles turned to be positive after the protein loading. The highest value was obtained when the nanoparticles were prepared under the same condition as those, which yielded the large particles. The zeta potential decreased, as the dextran concentration was increased and/or the polymerization time, at which BSA was loaded, was extended. It was noted that the nanoparticles prepared at this pH were widely distributed in their particle size.

The protein loading of nanoparticles polymerized at pH 3 was found to be comparable to one another, independent of the concentration of stabilizer. In contrast, the protein entrapment efficiency was reduced as dextran was incorporated. The reduction was not affected by the stabilizer concentration. In case of the polymerization at pH 1, the loading and the entrapment efficiency was varied, depending on both the concentration of dextran and the polymerization time, at which protein was loaded. The loading and the entrapment were high when the nanoparticles were prepared at lower dextran concentration of 5 and 10% w/v and BSA was loaded onto the nanaoparticles at hour 4 and 2 of polymerization, respectively. Both were reduced as the stabilizer concentration was increased and/or protein was loaded at the later time.

Polymerization at pH 3 without stabilizer resulted in the smooth spherical nanoparticles (Figure 4.5A). When 10% w/v dextran was added into the polymerization medium, the small and more uniform-sized nanoparticles were obtained (Figure 4.5B). An agglomeration of many small discrete nanoparticles was observed, as BSA was loaded onto the particles. The effect was more pronounced, when the stabilizer was included in the preparation process (Figure 4.5D-4.5E). Fabrication of the nanoparticles at pH 1 in the presence of 10% w/v dextran yielded the relatively large and partly-deformed particles, as depicted in Figure 4.5C. Incorporation of BSA obviously induced a massive agglomeration of nanoparticles (Figure 4.5F).

Table 4.3 Physicochemical properties of poly(lactic-co-glycolic acid) microparticles

	Blank microparticles		BSA-loaded microparticles			
	Size (μm)	Zeta potential (mV)	BSA loading (%)	EE* (%)	Size (μm)	Zeta potential (mV)
PLGA, 1% PVA	-	-	4.12 (0.07)	76.75	8.751 (1.460)**	-3.497 (24.57)***
PLGA, 2% PVA	0.938 (0.429)	-1.906 (4.360)	5.33 (0.58)	99.67	6.260 (1.810)	-2.673 (17.90)

*Entrapment efficiency

**Absolute deviation from the median (Uniformity)

***Standard deviation

Table 4.4 Physicochemical properties of poly(α-butyl cyanoacrylate) nanoparticles

	Blank nanoparticles		BSA-loaded nanoparticles			
	Size (μm)	Zeta potential (mV)	BSA loading (%)	EE* (%)	Size (μm)	Zeta potential (mV)
BCA 3.0	0.459 (0.104)**	-28.29 (7.254)***	3.58	32.23	0.848 (0.284)	-21.28 (4.647)
BCA 3.5	0.495 (0.186)	-23.55 (4.696)	3.74	19.34	0.900 (0.180)	-18.21 (3.682)
BCA 3.10	0.476 (0.030)	-17.56 (5.902)	3.43	20.28	0.930 (0.369)	-16.28 (4.692)
BCA 1.5	0.935 (0.528)	-2.211 (8.920)	9.51	97.16	6.343 (0.508)	32.98 (6.523)
BCA 1.10-2	0.796 (0.458)	-1.815 (5.678)	21.79	99.62	5.535 (0.330)	36.19 (8.439)
BCA 1.10-3	0.796 (0.458)	-1.815 (5.678)	5.70	46.34	0.222 (0.263)	26.55 (15.36)
BCA 1.10-4	0.796 (0.458)	-1.815 (5.678)	3.88	35.93	0.230 (0.312)	15.52 (10.84)
BCA 1.20	0.324 (0.402)	-2.745 (3.646)	1.70	27.66	0.161 (0.317)	5.697 (6.255)
BCA 1.30	0.296 (0.511)	-2.524 (3.677)	-	-	-	-

*Entrapment efficiency

**Polydispersity index

***Standard deviation

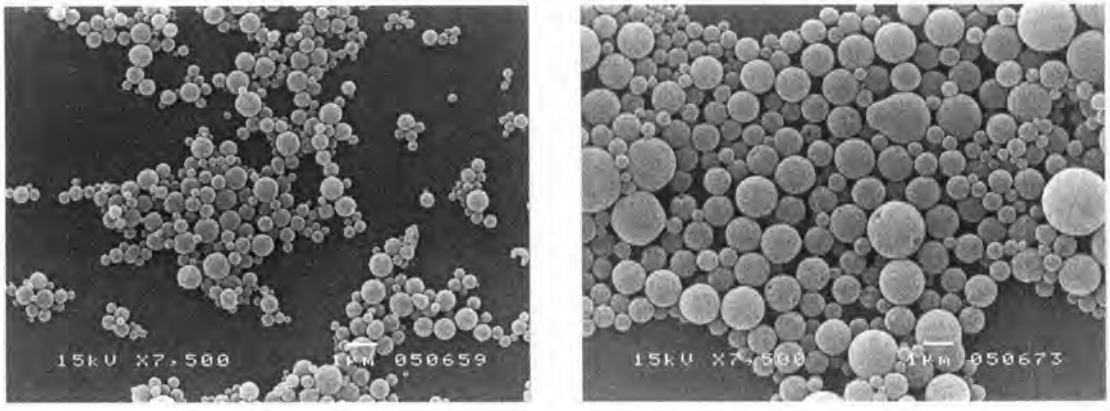

(A) (B)

Figure 4.4 Scanning electron photomicrographs of (A) blank and (B) BSA-loaded PLGA microparticles, prepared with 2% w/v PVA

Apart from the zeta potential, another surface property of micro-/nanoparticles was also investigated by XPS. The technique analyzes the type and the amount of elements exposed at the surface of materials. The results are shown in Table 4.5.

Upon incorporation of BSA into the LCS microparticles, the exposure of nitrogen on the surface of BSA-loaded microparticles was obviously increased, along with the appearance of sulfur exposure on the surface. About 60% of the particle surface was covered with BSA. Compared with the LCS microparticles, the nitrogen exposure on the surface of GEL LCS microparticles was also increased, indicating some deposition of GEL on the particle surface. Surprisingly, no exposure of sulfur was detected in this case. Therefore, it could be postulated that the appearance of sulfur exposure was resulted from the accumulation of BSA, which governed about 46% of the particle surface. In case of both blank and BSA-loaded POL LCS microparticles, the exposure of nitrogen on the particle surface was decreased remarkably. Meanwhile, the exposure of sulfur on the surface of BSA-loaded particles was also undetectable. It was thus conceivable that most of the particle surface was masked by POL. The exposure of nitrogen on the surface of blank EUD LCS microparticles was comparable to that of the blank LCS microparticles. Upon encapsulation of protein, only about 20% of the particle surface was deposited with BSA.

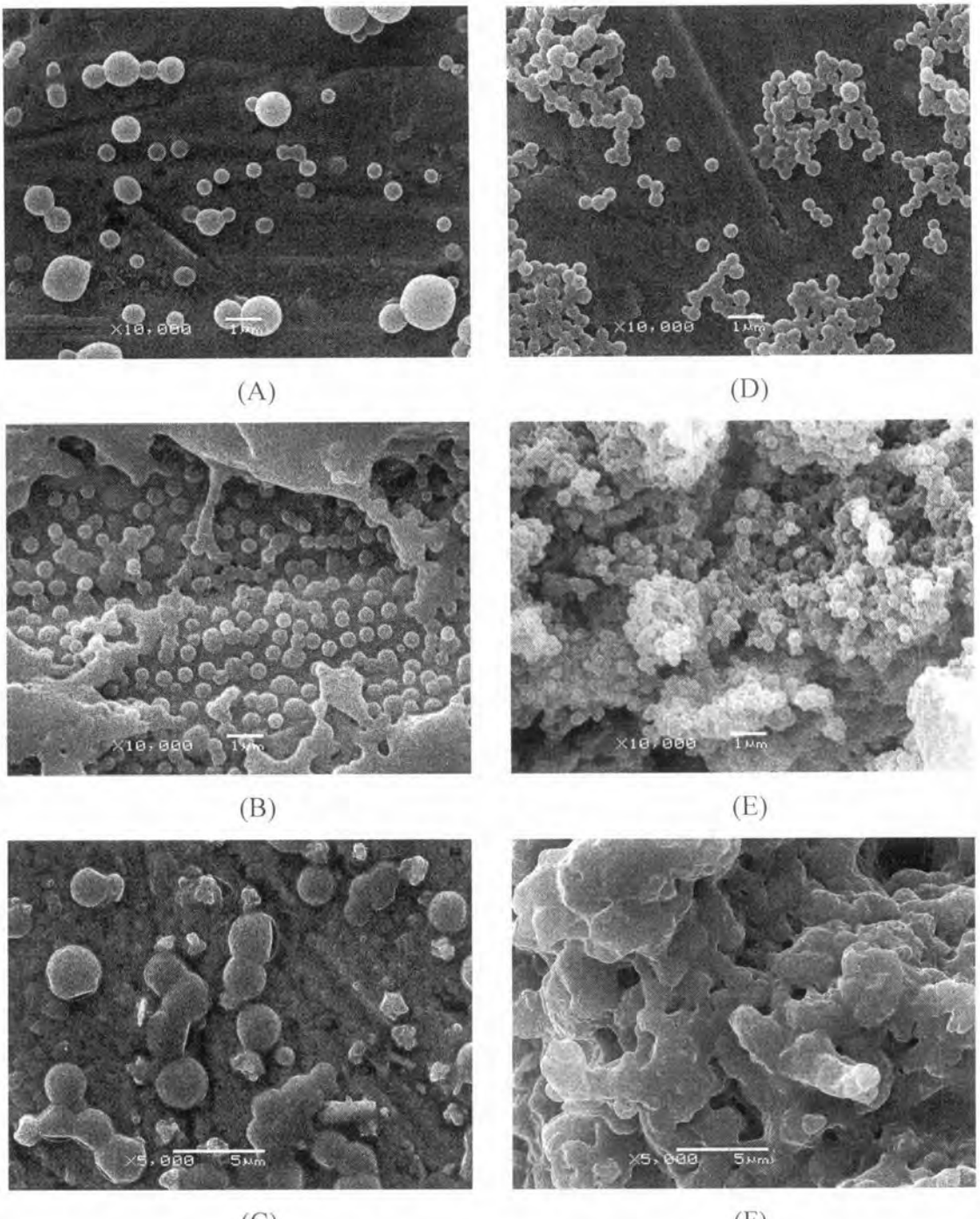

Figure 4.5 Scanning electron photomicrographs of blank BCA nanoparticles, prepared by anionic polymerization at (A) pH 3 without dextran, (B) pH 3 with 10% dextran, (C) pH 1 with 10% dextran, and BSA-loaded BCA nanoparticles, prepared at (D) pH 3 without dextran, (E) pH 3 with 10% dextran, and (F) pH 1 with 10% dextran and loaded with BSA at hour 4 of polymerization

Table 4.5 Percentage of elements exposed at and BSA coverage on the particle surface

Particles	Elements on blank particles (%)				Elements on BSA-loaded particles (%)					BSA coverage (%)
	C	O	N	Other	C	O	N	S	Other	
BSA					65.56	18.97	14.57	0.62	-	100.00
LCS	67.47	25.81	6.72	-	69.06	16.86	13.70	0.38	-	61.29
15 GEL LCS	65.89	18.09	16.02	-	66.90	18.22	14.59	0.29	-	46.77
15 POL LCS	74.40	24.71	0.89	-	71.36	26.88	1.76	-	-	-
15 EUD LCS	75.35	18.62	6.03	-	77.34	18.77	3.76	0.13	-	20.97
PLGA, 2% PVA	53.79	24.72	-	Si, 21.48	55.07	24.94	-	-	Si, 19.99	-
BCA 3.0					74.98	16.42	8.60	-	-	-
BCA 3.10					73.09	17.15	9.62	0.14	-	22.58
BCA 1.10-2					74.06	15.15	10.64	0.15	-	24.19
BCA 1.10-4					72.86	18.17	8.97	-	-	-

Surface composition of blank and BSA-loaded PLGA microparticles were alike. Furthermore, no exposure of sulfur was detected on the surface of protein-loaded particles. Thus, it was assumed that none of BSA was deposited on the particle surface. It was noticed that a significant amount of silicon was also found on the surface of microparticles.

Deposition of BSA on the surface of BCA nanoparticles was detected only on the surface of those prepared at pH 3 with 10% w/v of dextran and pH 1 with 10% w/v of dextran, on which BSA was loaded at hour 2 of polymerization. BSA coverage on the particle surface was about 20% for both nanoparticles.

***In vitro* release test**

The release of BSA from micro-/nanoparticles was performed *in vitro* in pH 7.4 PBS at 37 °C. The profiles are illustrated in Figure 4.6.

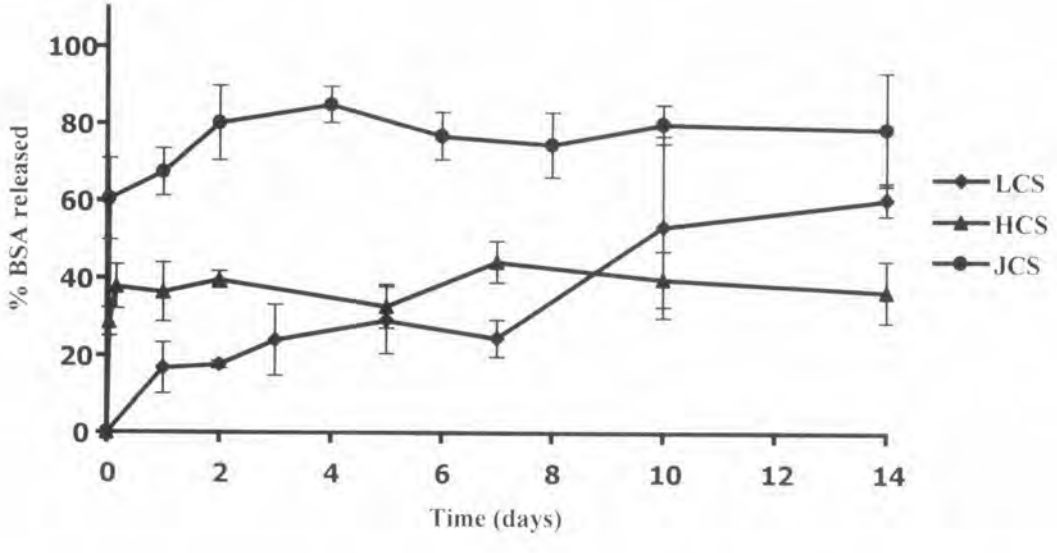

(A)

Figure 4.6 *In vitro* BSA released from (A) chitosan microparticles, (B) crosslinked and LCS composite microparticles, PLGA microparticles, and (C) BCA nanoparticles, as a function of time

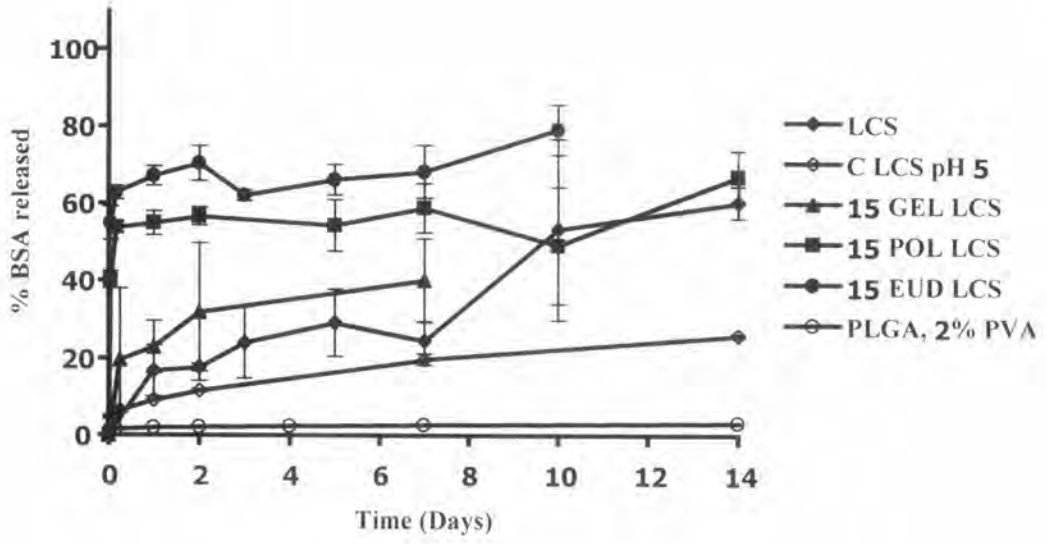

(B)

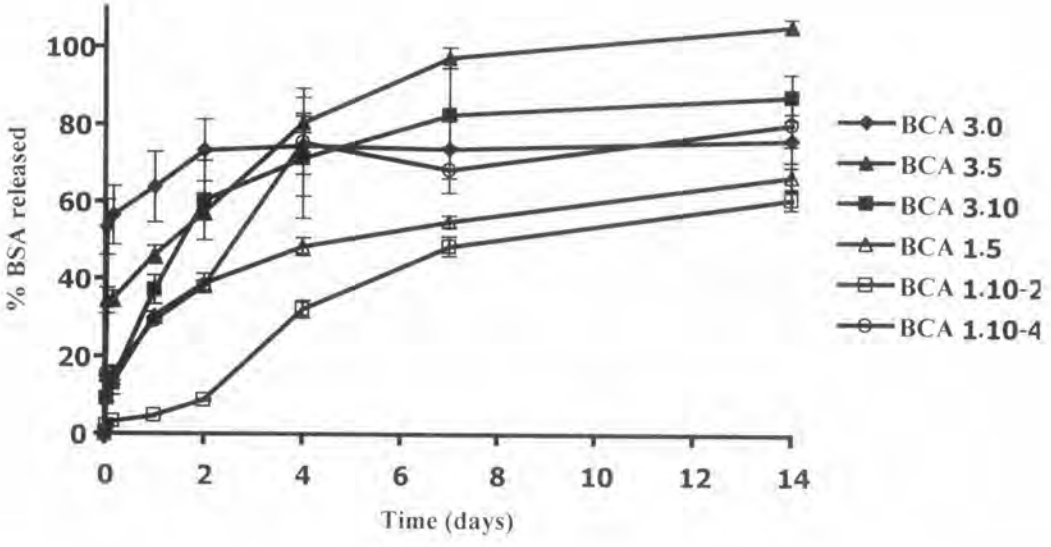

(C)

Figure 4.6 *In vitro* BSA released from (A) chitosan microparticles, (B) crosslinked and LCS composite microparticles, PLGA microparticles, and (C) BCA nanoparticles, as a function of time (continued)

While the LCS microparticles gradually released the protein throughout the time course of release study, the higher molecular weight of HCS and JCS microparticles burstly released BSA within a few hours. The maximum release was

reached at about 40 and 80% within the first and the second day of the test, for HCS and JCS microparticles, respectively (Figure 4.6A).

Modification of chitosan microparticles, either by co-spray drying with the excipients or cross-linking with the phosphate anions, changed the release behavior of BSA substantially. Incorporation of 5% w/w GEL yielded the similar release pattern to that of the LCS microparticles, but the maximum release was achieved only at about 15% within a few days (data not shown). Increasing the GEL concentration resulted in a faster release, along with the higher amount of liberated protein at the stable release phase (Figure 4.6B). The effect was more pronounced at high GEL concentration of 25% w/w (data not shown). POL and EUD induced a burst release of BSA out of the particles within a few hours and the stable phase of release was obtained within a day and a few days, respectively. Varying concentration of the excipients in microparticles did not affect the release profiles significantly (data not shown). It was noticed that the EUD composite microparticles yielded a little higher amount of protein released than the POL composite microparticles.

For HCS and JCS microparticles, the burst release on the first day was observed for all composite microparticles. Addition of either GEL or POL yielded almost the comparable release profiles to those of the original particles, except the GEL HCS microparticles, which released the protein about one-third more than the HCS microparticles. Incorporation of EUD induced a higher amount of BSA released than the original particles, with a greater extent for HCS microparticles (data not shown).

Cross-linking the LCS and the LCS composite microparticles resulted in the similar release profiles to one another, which were slow, but smooth for at least 4 weeks, except the crosslinked GEL LCS microparticles which achieved the maximum release of about 20% within the first day (data not shown).

PLGA microparticles released the protein most slowly, among the micro-/nanoparticles investigated in this study. Only about 3% of encapsulated protein was

released within 4 weeks (Figure 4.6B). The particles prepared with 1% w/v PVA gave the similar result (data not shown).

Generally, the protein adsorbed on the BCA nanoparticles prepared at pH 3 was released in a faster manner than those prepared at lower pH (Figure 4.6C). The BSA-loaded nanoparticles, fabricated without dextran, gave a burst release of protein and reached the maximum release within two days. Incorporation of dextran caused a slower release of protein. The higher the concentration of the stabilizer used during the preparation process, the slower release, along with the lower amount of BSA at the maximum release, was obtained. Both the stabilizer concentration and the polymerization time, at which protein was loaded, were found to influence the release pattern of protein from the nanoparticles prepared at pH 1. The particles, produced at 5 and 10% w/v dextran and loaded with BSA at hour 4 of polymerization (BCA 1.5 and BCA 1.10-4), released protein at the comparable rate, but those prepared at the higher concentration of stabilizer later released the higher amount of protein. Taking into account the polymerization time at protein loading (BCA 1.10-2 and BCA 1.10-4), the particles, on which protein was loaded at the later time, released BSA at a faster rate and seemed to achieve the maximum release at the higher amount of protein as well. As it could be expected, the nanoparticles produced at 20% w/v dextran also released BSA at the faster rate. About 55% of entrapped protein was released within two days and the maximum release was obtained at about 70% of the encapsulated protein (data not shown)

Integrity of encapsulated BSA

After the production, the integrity of encapsulated protein in all micro-/nanoparticles was confirmed by SDS-PAGE. It was apparent that neither the preparation process nor the composition of microparticles deteriorated the integrity of BSA. As illustrated in Figure 4.7, all bands of BSA, recovered from the microparticles moved downwards the electrophoretic gel in a comparable distance to the BSA in the molecular weight standard. No band was observed in either higher or lower molecular weight region, indicating that neither aggregate formation nor peptide backbone clipping occurred. Due to hydrophobicity of the BCA nanoparticles, the protein was extracted by shaking the nanoparticles in distilled water

overnight at room temperature. Unfortunately, the concentration of protein recovered from the BCA nanoparticles was probably too low to be visualized on the electrophoretic gel.

Smear appeared on the lanes of BSA-loaded chitosan microparticles was believed to be the staining of chitosan, since it was also found on the lane of blank chitosan microparticles.

Because all biological phenomena involve process of molecular recognition, it is essential that the delivery systems are able to release protein content in its native structure. Therefore, the structural conformation of BSA entrapped in the micro-/nanoparticles was investigated with CD. The CD spectra region of a single protein molecule can be observed within two regions, *i.e.* far ultraviolet (UV) (below 250 nm) and near-UV (250-300 nm) which correspond to secondary and tertiary structure of proteins, respectively (Kelly and Price, 1997; Sreerama and Woody, 2000). Unfortunately, concentration of BSA recovered from the micro-/nanoparticles was too low to reveal the CD spectra in the region of tertiary structure. Only investigation of secondary structure was then reported. BSA, which was recovered from the LCS and the HCS microparticles, yielded similar CD spectral shape to that of the unprocessed BSA (Figure 4.8A). All three spectra exhibit minima at *ca.* 208 and 222 nm, which were indicative of predominantly α-helical secondary structure (Pelton and McLean, 2000; Sreerama and Woody, 2000). It was noticed that the CD spectra of BSA recovered from the LCS and HCS microparticles showed lower molar ellipticity in some degree than that of the unprocessed BSA. In order to recover BSA incorporated in chitosan microparticles, it is inevitable that acidic solution had to be applied. It was reported in previous study that dissolving protein in acidic solution resulted in the decreased molar ellipticity in some degree, while the CD spectral shape was still maintained (Kusonwiriyawong et al., 2007). JCS as a raw material likely contained a trace component, which was able to absorb the polarized UV light (Figure 4.8A). In addition to the reduced molar ellipticity resulted from the acidic solution, the trace component also imparted some effect on the CD spectral shape, indicating a possible conformational change of the protein.

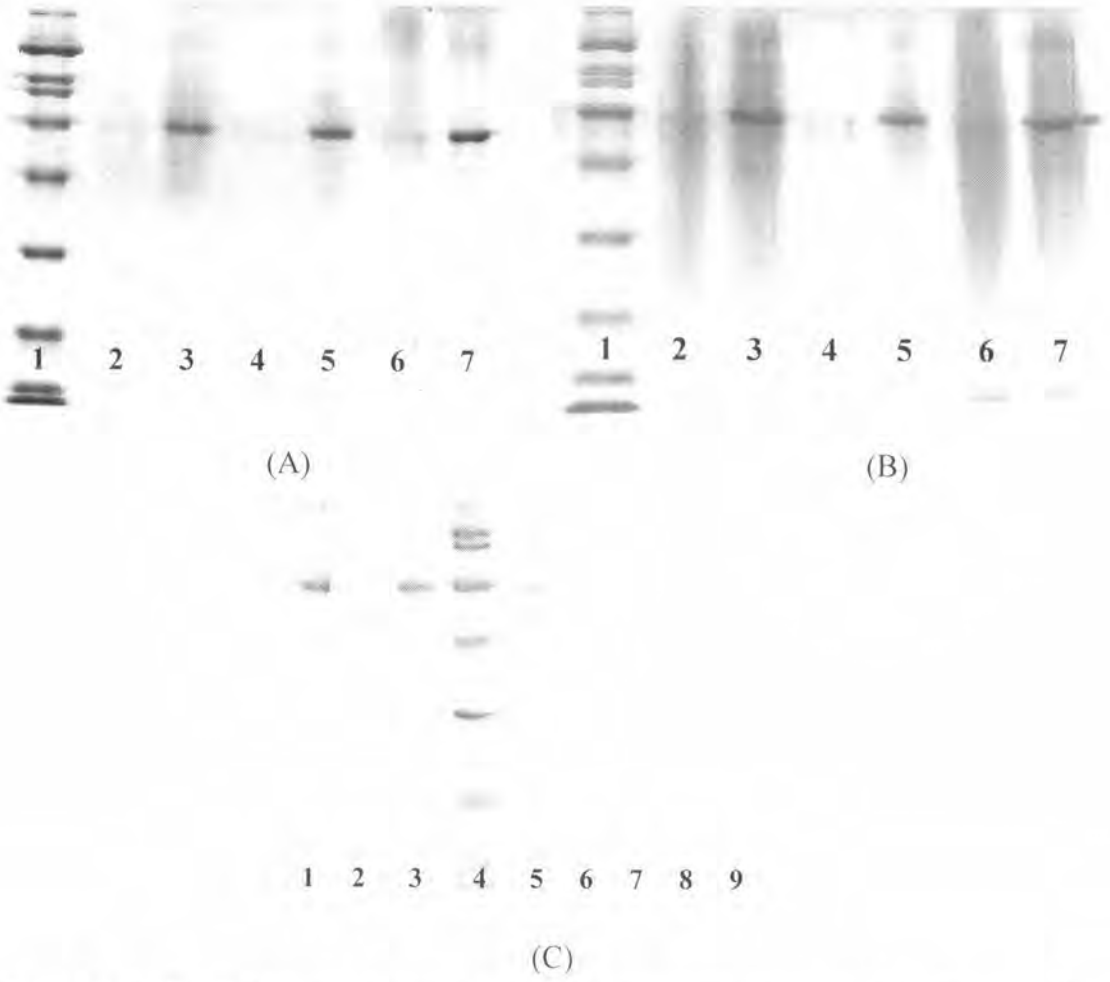

Figure 4.7 SDS-PAGE of (A) Lane 1: molecular weight standards, broad range (Bio-Rad Laboratories, Hercules CA, USA), Lanes 2 and 3: blank and BSA recovered from BSA-loaded LCS microparticles, Lanes 4 and 5: blank and BSA recovered from BSA-loaded HCS microparticles, Lanes 6 and 7: blank and BSA recovered from BSA-loaded JCS microparticles, (B) Lane 1: molecular weight standards, broad range, Lanes 2 and 3: blank and BSA recovered from BSA-loaded 15 GEL LCS microparticles, Lanes 4 and 5: blank and BSA recovered from BSA-loaded 15 POL LCS microparticles, Lanes 6 and 7: blank and BSA recovered from BSA-loaded 15 EUD LCS microparticles, and (C) Lane 1: unprocessed BSA, Lanes 2 and 3: blank and BSA recovered from BSA-loaded PLGA microparticles, Lane 4: molecular weight standards, broad range, Lane 5: 1.5 μg unprocessed BSA, BSA recovered from BSA-loaded Lane 6: BCA 3.0, Lane 7: BCA 3.5, Lane 8: BCA 3.10, Lane 9: BCA 1.10-4 nanoparticles

Incorporation of GEL into the LCS microparticles caused a substantial change of both the molar ellipticity and the CD spectral shape of encapsulated protein (Figure 4.8B). Depending on the GEL concentration, the effect was also varied. At 25% w/w GEL in the microparticles, the similar spectral shape and molar ellipticity of BSA were obtained, except that the position was shifted to the right (data not shown). In contrast, addition of POL and EUD did not affect the structural conformation of the entrapped protein significantly (Figure 4.8B). Furthermore, BSA recovered from the EUD-containing formulations seemed to be less susceptible to the acidic solution. Varying the concentration of both excipients in the microparticles also yielded the identical spectra to that of the corresponding composite microparticles (data not shown). In addition, modification of the HCS and the JCS microparticles by co-spray drying with the excipients caused the similar results to those of the LCS microparticles (data not shown).

In case of PLGA microparticles, the spectrum could not be obtained (Figure 4.8C). This indicated that α-helical secondary structure was lost in a great extent. Due to hydrophobicity of the BCA nanoparticles, the protein was extracted by shaking the nanoparticles in distilled water overnight at room temperature. Only BCA 3.5 could give an enough concentrated solution for the CD experiment. It was evident that CD spectrum of the recovered protein changed partly, in terms of both shape and molar ellipticity, from that of the unprocessed BSA (Figure 4.8C)

Cytotoxicity study

The micro-/nanoparticles were subjected to the cytotoxicity test with two antigen presenting cells. The effect of particle loading on viability of DC and Mϕ were depicted in Figures 4.9 and 4.10, respectively.

Typically, the percentage of cell viability increased as the particle loading was decreased. It was found that LCS microparticles were relatively non-toxic to DC (Figure 4.9A). The cytotoxicity profiles of HCS and JCS microparticles were shifted to the left, implying a slight increase in cytotoxicity. The 100% cell viability was found at the particle loading as high as 1 mg/ml for LCS and HCS microparticles, and

less than 0.1 mg/ml for JCS micropartilcles. The LC_{50} was calculated to be 8.79, 5.78, and 1.92 mg/ml for LCS, HCS, and JCS microparticles, respectively.

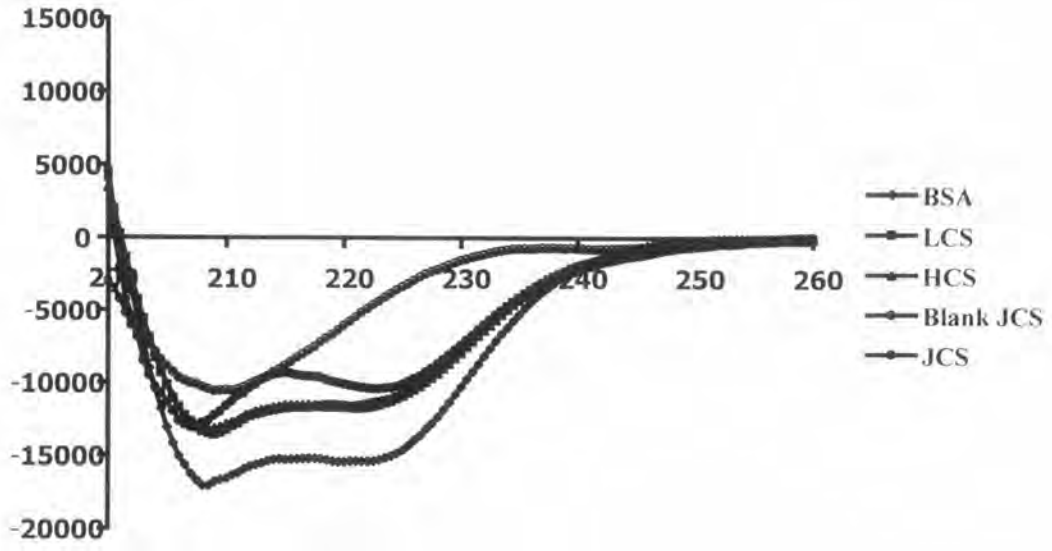

(A)

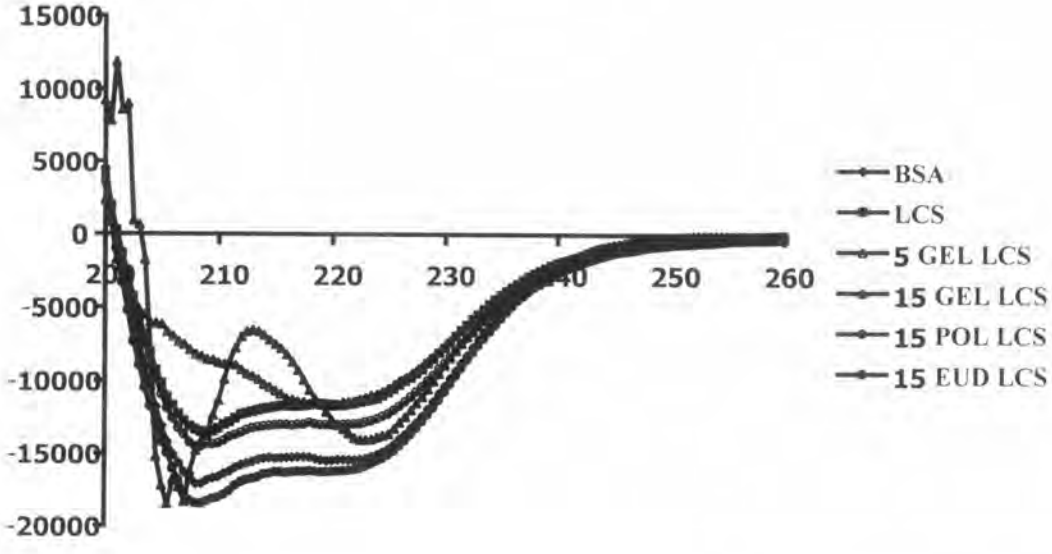

(B)

Figure 4.8 CD spectra of BSA recovered from BSA-loaded (A) chitosan microparticles of different molecular weights and sources, (B) chitosan composite microparticles, and (C) PLGA microparticles and BCA nanoparticles

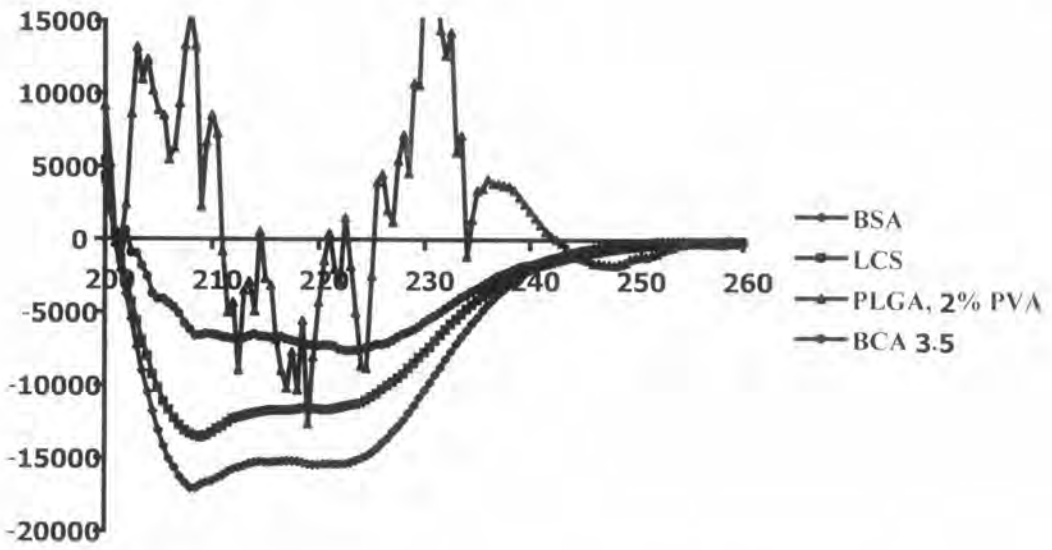

(C)

Figure 4.8 CD spectra of BSA recovered from BSA-loaded (A) chitosan microparticles of different molecular weights and sources, (B) chitosan composite microparticles, and (C) PLGA microparticles and BCA nanoparticles (continued)

The GEL LCS microparticles were a little more toxic to DC than the LCS microparticles, as the cytotoxicity profile was shifted slightly to the left (Figure 4.9B). Different concentrations of GEL in the microparticles also yielded the similar profiles to one another (data not shown). The 100% cell viability was obtained at the particle loading of 0.5 mg/ml for all GEL LCS microparticles. The LC_{50} was calculated to be 2.86, 1.77, and 5.60 mg/ml for 5, 15 and 25 GEL LCS microparticles, respectively. Incubation of the POL LCS microparticles with DC gave the comparable profile to that of the LCS microparticles. The results were not affected by the concentration of POL in the microparticles (data not shown). The LC_{50} was calculated to be 3.27, 4.97, and 8.40 mg/ml for 5, 15 and 25 POL LCS microparticles, respectively. Modification of HCS and JCS microparticles with GEL or POL yielded the similar cytotoxicity profiles to those of the original microparticles (data not shown). The LC_{50} was achieved at 4.33, 5.96, 1.44, and 3.15 mg/ml for the GEL HCS, POL HCS, GEL JCS, and POL JCS microparticles, respectively. As depicted in Figure 4.9B, all EUD composite microparticles and crosslinked LCS microparticles were apparently toxic to the cells. The 100% viability could not be obtained for all of these

microparticles within the investigated range of particle loading. The LC_{50} was ranged between 0.15-0.78 and 1.16 mg/ml for the EUD composite and crosslinked LCS microparticles, respectively.

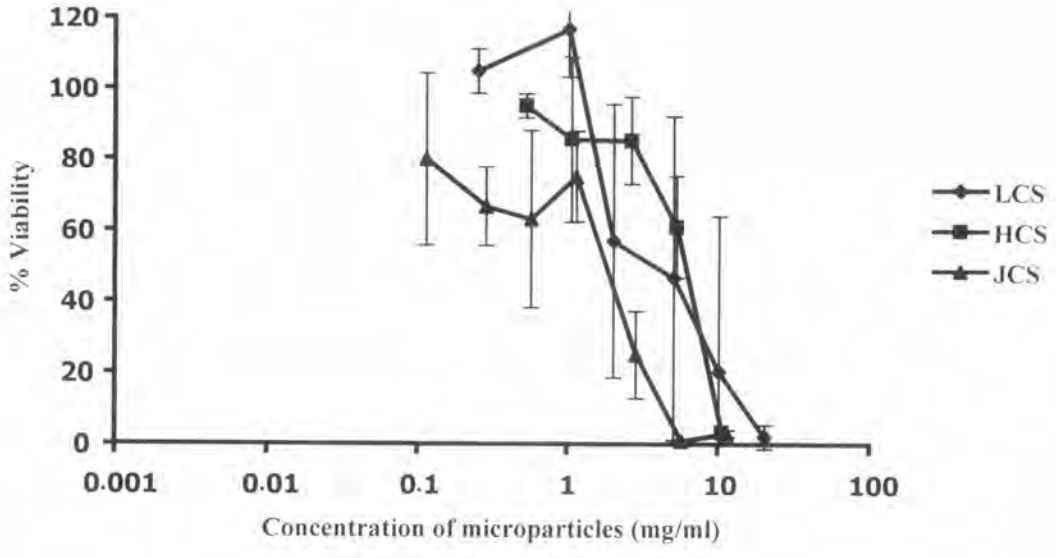

(A)

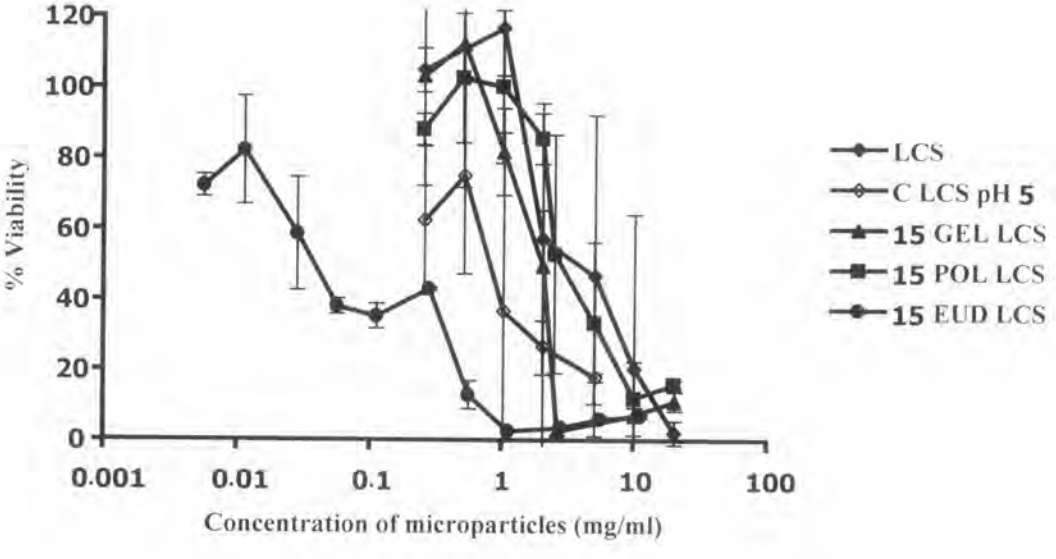

(B)

Figure 4.9 Percentage of dendritic cells' viability, co-incubated with (A) chitosan microparticles, (B) crosslinked and LCS composite microparticles, and (C) PLGA microparticles and BCA nanoparticles, as a function of micro-/nanoparticle loading

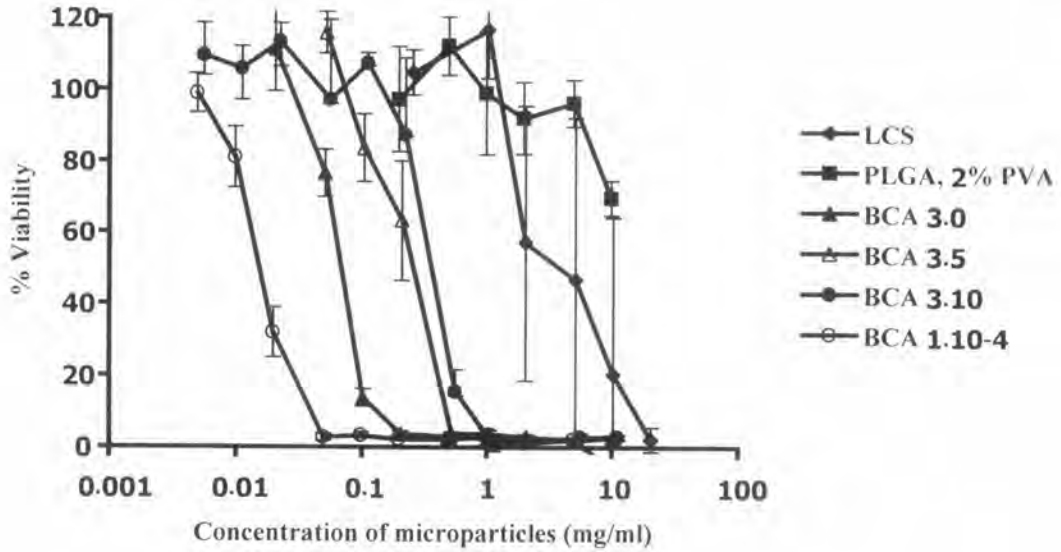

(C)

Figure 4.9 Percentage of dendritic cells' viability, co-incubated with (A) chitosan microparticles, (B) crosslinked and LCS composite microparticles, and (C) PLGA microparticles and BCA nanoparticles, as a function of micro-/nanoparticle loading (continued)

PLGA microparticles seemed to be non-toxic to DC within the studied range of particle loading. The 100% cell viability and the LC_{50} was obtained at the particle loading as high as 5 and 16.78 mg/ml, respectively. In contrast, the BCA nanoparticles were clearly toxic to DC. The 100% cell viability was obtained at the particle loading of 0.02, 0.5, 0.1, and 0.005 mg/ml and the LC_{50} was 0.10, 0.31, 0.54, and 0.02 for BCA 3.0, BCA 3.5, BCA 3.10, and BCA 1.10-4, respectively.

The viability test for Mϕ was mainly aimed at identifying the particle loading, which was not toxic to the cells, by applying the information obtained from the test with DC. Thus, the LC_{50} would not be determined for most cases. It was found that Mϕ seemed to be more susceptible to the micro-/nanoparticles than DC. Among the tested chitosan microparticles, the LCS microparitcles were still the least toxic to Mϕ. In contrast to the results of DC, the HCS microparticles were found to be slightly more toxic to Mϕ than the JCS microparticles (Figure 4.10A).

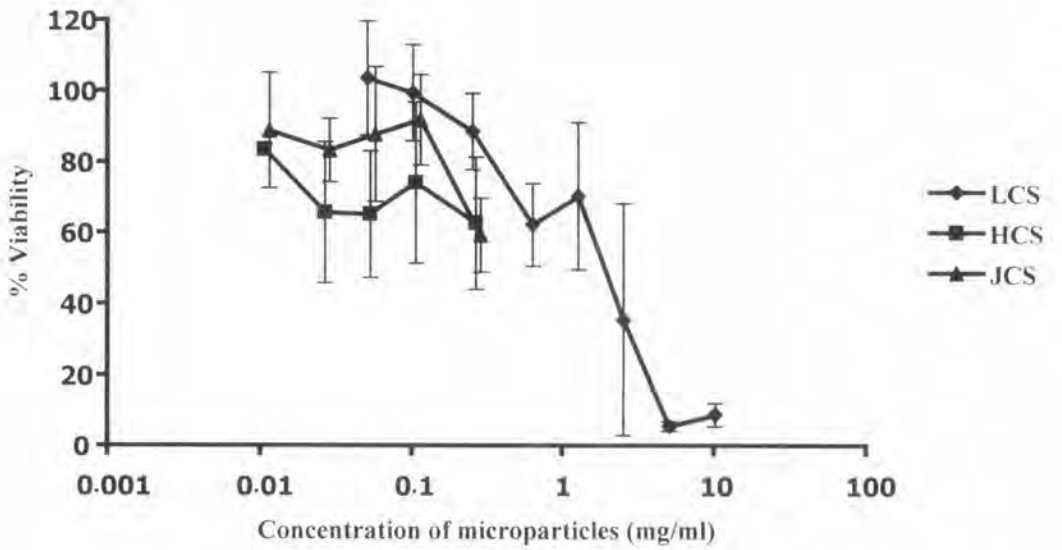

(A)

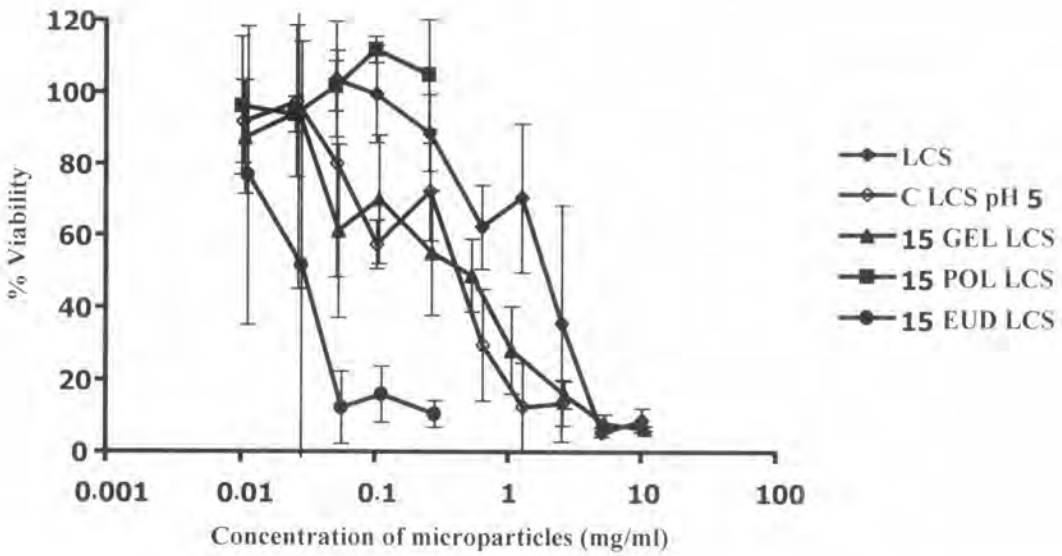

(B)

Figure 4.10 Percentage of macrophages' viability, co-incubated with (A) chitosan microparticles, and (B) crosslinked and LCS composite microparticles, as a function of micro-/nanoparticle loading

The GEL LCS microparticles were a little more toxic to Mϕ than the LCS microparticles, as it was evident by the shift of the cytotoxicity profile to the left. Varying the concentration of GEL in the microparticles did not change the profiles significantly (data not shown). At the particle loading of lower than 0.25 mg/ml, all

the POL LCS microparticles yielded the similar profiles to that of the LCS microparticles. As it was expected, the EUD composite microparticles were relatively toxic to Mϕ. The 100% viability could not be obtained for all of these microparticles within the investigated range of particle loading. In contrast to the result found with DC, the crosslinked LCS microparticles surprisingly produced a comparable cytotoxicity profile to that of the GEL LCS microparticles (Figure 4.10B).

Similar to the results obtained with DC, PLGA microparticles seemed to be non-toxic to Mϕ within the studied range of particle loading, *i.e.* lower than 0.25 mg/ml. The BCA nanoparticles were apparently toxic to the cells. The non-toxic particle loading was obtained at lower than 0.01 mg/ml for all investigated BCA nanoparticles (data not shown).

***In vitro* cellular uptake**

The prospective micro-/nanoparticles were labeled with FITC and incubated with the antigen presenting cells at the particle loading which was non-toxic to the cells. The cellular uptake was detected by FACS analysis. The results are shown in Table 4.6.

About 44-46% of DC was detected as positive for taking up the LCS and LCS composite microparticles. Except for the 15 POL LCS microparticles, as high as 74% of DC was defined as positive. The HCS and JCS microparticles were taken up at a lower extent than the LCS microparticles. When the microparticles were modified with GEL and POL, the cellular uptake was improved for POL HCS and JCS composite microparticles, while it was lower for GEL HCS microparticles. It was evident that the uptake of PLGA microparticles and BCA nanoparticles were lower than that of the LCS and LCS composite microparticles, but comparable to that of the HCS and JCS composite microparticles.

Mϕ was obviously more active in taking up the micro-/nanoparticles than DC. More than 60% of the cells were positive for the uptake of all microparticles, except the JCS microparticles, for which only about 47% of Mϕ were detected as positive.

PLGA microparticles and BCA nanoparticles were less efficiently taken up by Mϕ, when compared with the microparticles of chitosan derivatives. However, the uptake was still higher than that by the DC.

Table 4.6 *In vitro* cellular uptake of micro-/nanoparticles, as percentage of cells taking up the particles

Particles	Dendritic cells (%)	Macrophage (%)
BSA	34.96	5.51
LCS	49.00	80.65
5 GEL LCS	46.62	72.25
15 GEL LCS	44.61	68.24
25 GEL LCS	44.52	84.65
5 POL LCS	49.61	86.30
15 POL LCS	74.45	79.33
25 POL LCS	45.47	76.52
HCS	32.57	73.95
15 GEL HCS	25.59	69.76
15 POL HCS	37.47	77.24
JCS	27.39	47.49
15 GEL JCS	38.12	63.00
15 POL JCS	39.56	74.51
PLGA, 2% PVA	30.42	37.96
BCA 3.5	32.66	43.34
BCA 3.10	33.97	42.76

Discussion

The biodegradable and biocompatible micro-/nanoparticles intended for cellular delivery of protein were prepared from three different types of polymer. The aqueous acidic solution of chitosan was spray dried under a controlled condition. The

microparticles of different molecular weights and sources did not differ apparently in terms of physicochemical characteristics and morphology. The properties of microparticles were modified by co-spray drying with the acceptable pharmaceutical excipients. GEL was included because it has been used as a stabilizer in several vaccine formulations (Barbour *et al.*, 2002; Sarkar *et al.*, 2003). Interestingly, it conferred higher positive zeta potential to the chitosan microparticles, which might enhance the particle uptake by DC and Mϕ (Foged *et al.*, 2005; Thiele *et al.*, 2001). It was reported that, by addition of a non-ionic surfactant, the protein accumulation at the air-liquid interface of the droplets during spray drying was reduced and hence the residual activity of encapsulated protein was increased (Millqvist-Fureby, Malmsten and Bergenståhl, 1999; Sturesson and Carlfors, 2000). The incorporation of POL was thus intended for retention of protein stability. Although POL tended to adsorb at the particle surface and likely affected the surface property of particles, the zeta potential of the POL LCS microparticles was surprisingly comparable to that of the LCS microparticles. However, the accumulation of POL at the particle surface obviously affected the morphology and topography of microparticles. Due to its low melting point at about 56 °C (Collett and Weller, 1994), POL likely melted under the drying temperature and bound the adjacent microparticles together upon later solidification. The agglomeration of particles was thus obtained. EUD, a cationic derivative of poly(acrylic acid), was co-spray dried with chitosan since it holds the pH-dependent membrane-disruptive property, which is very beneficial for delivery of protein to the cytosol (Kusonwiriyawong *et al.* 2003). Unlike the polycationic GEL, EUD did not apparently affect the zeta potential of microparticles. In addition, a good appearance of microparticles was also achieved, attributed to its good film-forming properties.

Surface modification of chitosan and chitosan composite microparticles by ionic cross-linking with tripolyphosphate anion resulted in a considerable change of both physicochemical properties and morphology of the particles. Due to weak acidic characteristics, the mean charge number and charge density of tripolyphosphate increased as pH of the solution was increased. In contrast, the ionization of amino group of chitosan, as a weak polybase, decreased with the pH increasing. Therefore, the optimal electrostatic interaction between tripolyphosphate and chitosan would

exist only at a certain pH range (Shu and Zhu, 2001). The cross-linking of LCS microparticles was then performed at pH about 9 of the original tripolyphosphate solution, where a partial cross-linking was expected, and at pH about 5, where an optimal cross-linking was likely obtained (Ko *et al.*, 2002). However, it was postulated that the LCS microparticles were crosslinked to a comparable extent at both processing pH, since the zeta potential was neutralized to the comparable value. Because of the polycationic nature, GEL in the composite microparticles likely interfered or even participated in the cross-linking reaction in one way or another, resulting in the agglomeration of several deformed microparticles. The accumulation of POL and the formation of EUD film at the particle surface might impede the cross-linking process in some degrees, according to the zeta potential of the resultant particles. Nevertheless, the smooth spherical microparticles were still obtained.

It was obvious from the analysis of particle surface compositions that the protein was a surface-active molecule and tended to adsorb at the particle surface (Adler and Lee, 1999; Fäldt and Bergenståhl, 1994; Landström *et al.*, 1999; Millqvist-Fureby *et al.*, 1999). All the excipients applied were found to compete against BSA for the accumulation at the particle surface, especially POL, which was able to replace BSA totally.

The 'burst effect' during first stage of the release test was quite common for chitosan microparticles (He, Davis and Illum, 1999). Generally, the higher molecular weight chitosan released the encapsulated drug more slowly than the lower one (Ko *et al.*, 2002). However, the opposite result was found in this study, even though the maximal release obtained from the higher molecular weight chitosan was still lower than that achieved from the lower one. Chitosan of similar properties, but from different sources, clearly yielded the different release behavior of the encapsulated protein. Incorporation of the excipients into microparticles mostly increased the release rate of BSA, possibly due to their aqueous solubility. Nevertheless, the maximal release did not differ significantly from that obtained from the original microparticles. Cross-linking of chitosan microparticles with polyphosphate anions resulted in a surface coat of tripolyphosphate/chitosan complex, which could hardly be dissociated (Shu and Zhu, 2002). Consequently, the retarded release of BSA was

gained. The reaction could be interfered by the formulation component that could donate the ionic charge, as previously described.

The integrity of BSA was obviously maintained after encapsulation into all types of investigated chitosan microparticles. However, the trace component existed in the chitosan from international source or any excipient incorporated into the microparticles could affect the conformational structure of the encapsulated protein as well.

PLGA microparticles, with a very good appearance, were prepared by double-emulsion solvent-evaporation method. The resultant microparticles were considered neutral. Due to the hydrophobicity and relatively high molecular weight of the polymer, the slow release of entrapped protein was obtained. The incorporated protein likely existed only in the internal aqueous phase and was entrapped *in situ* upon the particle formation. As a consequence, the deposition on the particle surface was undetectable. The preparation of microparticles essentially required the use of organic solvents as well as the sonication, which obviously imposed deleterious effects on the conformational structure and possibly the activity of encapsulated proteins (Cegnar *et al.*, 2004; van de Weert *et al.*, 2000).

BCA nanoparticles were prepared by anionic polymerization in aqueous media. The initiation of reaction occurs via hydroxyl anion, the rate of which could be then controlled by regulating pH of the polymerization medium (Behan and Birkinshaw, 2000). At pH above 5, the very rapid polymerization occurred, resulting in the formation of large unstructured agglomerates. The optimum pH for particle production was ranged between 2.25-3.5 (Behan, Birkinshaw and Clarke, 2001). However, some authors reported that the reaction could be well controlled at pH 1 (Chauvierre *et al.*, 2003). Incorporation of a steric stabilizer such as dextran could enchance the stability of polymerizing dispersions (Behan and Birkinshaw, 2000). It was found in this study that, without the stabilizer, the nanoparticles could be obtained by preparation only at pH 3, but not at pH 1. The reaction at pH 1 was likely too slow. Without the steric stabilizer, the forming particles could coalesce together, resulting in the formation of unstructured agglomerates. The stabilizer possibly

contained the forming particles until the complete formation could be achieved. As a consequence, increasing the concentration of stabilizer resulted in the formation of smaller nanoparticles. Upon incorporation of proteins, the anionic sites on the structural backbone of proteins could rapidly initiate or even participate in the polymerization process, leading to the agglomerate formation (Behan and Birkinshaw, 2001). Therefore, the proteins should be introduced once the particle formation was complete. It was evident that the complete formation of nanoparticles was hour 1 and after hour 4 of polymerization for the preparation at pH 3 and 1, respectively. Nevertheless, some agglomeration was still found. Most of BSA probably adsorbed onto the nanoparticles by hydrophobic interaction, which would less likely affect the integrity of protein. However, the conformational change of the protein structure was noticed. This probably resulted from the interaction between protein and forming particles upon the introduction of protein.

Chitosan was considered as a safe material (Illum, 1998). The products obtained from a local manufacturer yielded a comparable cytotoxicity profile, while that of the foreign source was a little more toxic, probably due to the trace component found in the CD study. Incorporation of the excipients did not affect the cytotoxicity profile of the particles significantly, except EUD, which was obviously toxic to the cells. It was reported to own the pH-dependent hemolytic activity at the concentration as low as 1.9 μg/ml (Kusonwiriyawong *et al.*, 2003). In this study, at the particle loading of 0.01 mg/ml, which was equivalent to EUD about 1.5 μg/ml, the toxic effect was still found (about 80% cell viability). Furthermore, the crosslinked particles were also toxic to the cells. It was possible that some trace amounts of polyphosphate anions disturbed the buffer system of cell culture. While the PLGA microparticles were less toxic to the cells than the chitosan microparticles, the BCA nanoparticles were more toxic. This was likely caused by the cytotoxic compounds from the degrading nanoparticles (Lherm *et al.*, 1992).

It was conceivable that the particle size might be the most important factor in determining the uptake capacity. For the LCS and the composite microparticles, the uptake by both cells was comparble. As the particle size of microparticles was

slightly larger for the HCS and the JCS microparticles, the uptake was also slightly reduced. The PLGA microparticles and the BCA nanoparticles, which held the particle size close to the most appropriate size range of 1-2 μm for the uptake by macrophages (Tabata and Ikada, 1988), were less taken up than the chitosan microparticles. This likely resulted from the exposed negative charge on the particle surface (Thiele *et al.* 2001).

Conclusion

The micro-/nanoparticles of chitosan, poly(lactic-co-glycolic acid), and poly(α-butyl cyanoacrylate), which represented the cationic, neutral, and anionic particles, respectively, intended for cellular delivery of proteins were successfully prepared. Modification of the chitosan microparticles either by co-spray drying with the acceptable pharmaceutical excipients or ionically cross-linking with the polyphosphate anions resulted in the particles with varied physicochemical properties and/or biological properties. All chitosan and chitosan composite microparticles exposed positive zeta potential and were relatively non-toxic to both DC and Mϕ, except the EUD composite microparticles, which were quite toxic to both cells. Cross-linking the surface of chitosan microparticles also resulted in the increased cytoxicity. Poly(lactic-co-glycolic acid) microparticles were relatively neutral and non-toxic to the cells. In contrast, the negatively-charged poly(α-butyl cyanoacrylate) nanoparticles were toxic to both DC and Mϕ. The chitosan, the GEL and the POL composite microparticles were efficiently taken up by both antigen presenting cells. All the prospective chitosan microparticles will be further investigated as the potential delivery systems for targeting vaccine antigen to the antigen presenting cells.